Spatiotemporal Analysis of Air Temperature Indices, Aridity Conditions and Precipitation in Iran

Amin Sadeqi (✉ aminn19@gmail.com)
   University of Tabriz   https://orcid.org/0000-0001-7717-9086

Ercan Kahya
   Istanbul Technical University

Abstract

Global warming has become a major threat to life on the earth, and recognizing its impacts can definitely be useful in controlling and mitigating its adverse effects. In this study, time series variations in air temperature indices (frost days, T_{min}, T_{max}, T_{mean}, T_{minmin}, T_{maxmax}, $T_{soil-min}$), De Martonne aridity index (I_{DM}) and total precipitation were investigated using a long-term meteorological data (1960−2019) of 31 synoptic stations throughout Iran. The results indicated that more than 94% of the stations had increasing trend in T_{mean}, in which about 70% were significant at the 0.05 level. The average increase in T_{min} was calculated approximately 1.7 times higher than T_{max} and also the increase in T_{minmin} was about 2.5 times higher than T_{maxmax}. Our findings showed that, abrupt changes in T_{min} and T_{max} mostly observed in the 1990s were upward in 87% of all the stations. Increase in annual T_{mean} at a rate of 0.3 °C per decade and reduction of 5 mm per decade in total annual precipitation led to decrease in the I_{DM} aridity index by 0.35 per decade in Iran. The intensity of air temperature increase was higher in tropical regions than in cold regions. Trend analysis in the partial series before and after a change point showed that the trends in T_{mean} before the change point were negative, but turned to positive afterwards in some stations mostly located in the northwestern cold and mountainous regions of the country. Our results revealed that the climate in Iran, in general, has become warmer and drier in the past 60 years and continuation of the current global warming trend will exacerbate this problem in the future.

Highlights

- Iran has become warmer and drier over the last six decades.
- Global warming has caused the average annual T_{min} to experience three significant abrupt upward changes in their time series at some stations.
- The time series trend of some indices before the change point was different than their trend afterwards.
- The east coast of the Caspian Sea has shifted from Mediterranean region to semi-arid region due to climate change.
- Tropical regions were warmed more intense than cold regions.

1. Introduction

Air temperature plays an important role in the interaction of the Earth's climate system. Surface air temperature has risen over the past century due to human activities via excessive emissions of greenhouse gases into the atmosphere (IPCC 2013). Global warming has also led to changes in other climatic variables, which has brought about fundamental concerns toward environment as well as anthropogenic issues. The regional advent of global climate variation does not often conform to the behaviour of global mean temperature (Pokorná et al. 2018). In other words, the effects of climate change have been shown to differ from region to region (IPCC 2014). It is then important to identify the

cause of such events as well as searching the existence of some signs or particular periodicities in data of interest.

An increase of 1°C in global temperature leads to approximately 1.5 to 2 % increase in the global mean precipitation and about 4% increase in the global surface runoff (Labat et al. 2004; Salzmann 2016). In the same context, each 1°C further increase in temperature may, on the average, cause to decrease global wheat production by 6% (Asseng et al. 2014). Similarly, Sinha et al. (2020) demonstrated that a rise of 2°C in the global mean surface air temperature will confront an additional 15% of the global population under water scarcity condition. Lenton et al. (2017) showed increasing monthly temperature variability and autocorrelation in large parts of northern hemisphere. Estrada et al. (2017) discovered that, since 2000, the accumulated total costs caused by the impacts of global and local climate change were about 2.6 times greater than the costs without urban-weather-related factors in every city all over the world.

In the second half of the 20th century, warming in the Middle East regions was greater than the global warming. These regions are, therefore, propounded as potential hot-spots due to climate change (Mostafa et al. 2019; van Oldenborgh et al. 2009). Having an area of 1.648 million km² and a population of about 82 million, Iran is one of the largest countries in the Middle East ranked as the second most populous country in the region after Egypt, along with Turkey. The vulnerability to the climate change impacts is more pronounced in developing countries, such as Iran, which are heavily dependent on their natural resources and communities with high social diversities.

Since relating the variability of regional surface variables to the large-scale atmospheric circulations have been a common practice in last several decades, Kahya (2011) reported that North Atlantic Oscillation (NAO), a dominant mode of Atlantic sector climate variability, has the far-field influence on interannual to decadal variations in main climate and hydrological variables in the eastern Mediterranean region. For example, Dezfuli et al. (2010) studied the regional rainfall teleconnections to the Southern Oscillation (SO) and NAO at the seasonal time scale to search regional drought predictors across the southwest Iran. They found that the NAO is negatively correlated with autumn rainfall such that it is least likely for an extreme autumn drought to occur when June-August NAO is negative. Dezfuli et al. (2010) concluded that, similar to droughts, the wet winter seasons were not significantly in association with either SO or NAO. Vazifehkhah and Kahya (2018) focused on the influences of winter NAO and Arctic Oscillation (AO) extreme phases on hydrological drought using a standardized streamflow index (SSFI) over Turkey and northern Iran. The outputs of SSFI for the positive extreme phases of NAO and AO appeared to notably different in Turkey and Iran in such a way that multiple drought events were detected in Turkey for all timescales as, in most cases, opposed to those in Iran. The regions in the western and eastern Turkey were exposed to drought conditions in various magnitudes during the positive extreme phases of NAO whereas fewer droughts were observed in Iran around the Caspian Sea during the negative NAO and AO extreme phases.

In a close geography, Vazifehkhah and Kahya (2019) investigated hydrological and agricultural droughts and their characteristics using the Standardized Streamflow Index (SSFI) and Standardized Soil Moisture

Index (SSI) across the Konya Closed Basin in Turkey, respectively. They also analysed the teleconnections of various large-scale climate indices (e.g., NAO, AO) over 3-month SSFI and SSI series applying cross wavelet transform and pointed out an increase in drought duration and severity in the basin since 1999. In a proceeding study (Vazifehkhah et al. 2019), they were concerned with non-parametric multivariate standardized drought index (NMSDI) based on precipitation and soil moisture data in conjunction with copula functions in the same basin. The bivariate return period analysis of the NMSDI using the two typical drought characteristics (duration and severity) resulted in a high risk for southeastern and southwestern parts of the basin for the 3-month NMSDI series while north to northwestern parts could be exposed to high risk for the 6-month series.

Precipitation and air temperature are two most influential and crucial variables in climatic and hydrological studies. Changes in precipitation and air temperature sharply alter the hydrological cycle; therefore, trend and abrupt change detection analysis in rainfall and temperature patterns is important in understanding climate dynamics. A rigorous precipitation time series analysis provides us a better understanding of changes in the aridity index. In this study, we aimed to examine air temperature indices and I_{DM} aridity index time series in Iran using non-parametric methods to achieve the following objectives:

(i) To analyse air temperature time series variables including average daily minimum air temperature (T_{min}), average daily maximum air temperature (T_{max}), mean daily air temperature (T_{mean}), absolute minimum air temperature (T_{minmin}), absolute maximum air temperature (T_{maxmax}), mean daily minimum soil surface temperature ($T_{soil-min}$), and finally frost days (FD: defined as the number of days with minimum daily temperature below 0°C) in association with the influences of climate change;

(ii) To explore changes in aridity conditions using modified De Martonne aridity index;

As far as is known, the determination of changes in climate is a prerequisite for a better understanding of the climate and developing adaptation and mitigation measures at regional and local scales (Gebrechorkos et al. 2019). Upon an overall review on previous studies, it is said that none has been focused on monotonic trends in climate variables during a long-term period like more than 50 years in Iran. The potential of more than one break points in a climate time series, at the first time, has been of primary interest in this study. In addition, the trends before and after the breakpoints has been also considered for accurate pertinent inferences in this study. Our results can be applicable in managements of water resources and agriculture.

2. Materials And Methods

2.1. Study area and data

Iran is located in the Middle East region between 25° 00´ to 39° 47´ N and 44° 02´ to 63° 20´ E, and covers almost 1.1% of the world's land area (Fig. 1 and Table 1). Studies concerning climate change require long-term data, which are usually limited in Iran. Absence of recorded data in the country

influences climate change studies and it is also a main limiting factor for impact assessments and policy-making processes. In this research, climate data were collected from Iran Meteorological Organization, IRIMO (https://data.irimo.ir/). Many synoptic stations in Iran are newly established and do not have a long-term record. We first selected a set of the stations having observations since 1960 among more than 300 synoptic stations, and later excluded those with more than 10% missing observations among the remaining stations. Finally, we identified 31 synoptic stations that had a long-term recorded data for the last 60-year period (1960–2019). Hence the records of $T_{soil-min}$ since 1970 is only available data, the $T_{soil-min}$ was analysed for the period 1970–2019. It is worthwhile to mention that we used 65 extra synoptic stations for the spatial distribution maps. In other words, we used 96 stations that covered all the extent of Iran for the last decade (2009–2018) only for extracting interpolation maps.

Table 1
Climatic characteristics of the synoptic stations used in this study

No.	Station name	Region	Rainfall (mm)		Air temperature (ºC)		Climate condition
			mean	SD	mean	SD	
1	Esfahan	Central area	123	49	16.4	0.7	HA
2	Kerman	Central area	136	47	16.0	0.9	A
3	Shiraz	Central area	311	107	17.9	0.9	SA
4	Yazd	Central area	56	26	19.5	1.0	HA
5	Anzali	Coastal area across Caspian Sea (North)	1780	345	16.4	0.8	HHB
6	Babolsar	Coastal area across Caspian Sea (North)	890	166	17.2	0.8	H
7	Gorgan	Coastal area across Caspian Sea (North)	569	123	17.9	0.7	M
8	Ramsar	Coastal area across Caspian Sea (North)	1227	280	16.3	0.8	HHA
9	Rasht	Coastal area across Caspian Sea (North)	1332	260	16.2	0.9	HHA
10	Bandarabbas	Coastal area across Persian Gulf and Oman Sea	169	111	27.0	0.6	HA
11	Bushehr	Coastal area across Persian Gulf and Oman Sea	242	111	24.8	0.8	A
12	Birjand	East	160	51	16.6	0.8	A
13	Abadan	South West (Khuzestan plain)	153	62	25.7	1.0	HA
14	Ahvaz	South West (Khuzestan plain)	223	86	25.6	1.0	A
15	Mashhad	North East (Khorasan province)	249	69	14.6	1.3	SA
16	Sabzevar	North East (Khorasan province)	186	62	17.7	1.1	A
17	Torbat H.	North East (Khorasan province)	257	80	14.4	0.8	SA
18	Khoy	North West	293	81	12.2	1.3	SA
19	Orumiyeh	North West	331	97	11.6	1.1	SA
20	Tabriz	North West	282	80	12.7	1.0	SA

All the above indices are averaged over the last 60-year period from 1960 to 2019. Furthermore, SD denotes standard deviation.

No.	Station name	Region	Rainfall (mm)		Air temperature (ºC)		Climate condition
			mean	SD	mean	SD	
21	Zanjan	North West	303	78	11.3	1.1	SA
22	Bam	South East	57	26	23.3	1.0	HA
23	Zahedan	South East	80	40	18.6	0.8	HA
24	Qazvin	South side of Alborz mountains	315	85	14.2	1.1	SA
25	Shahrud	South side of Alborz mountains	156	54	14.8	0.9	A
26	Tehran	South side of Alborz mountains	232	72	17.6	1.0	A
27	Arak	Zagros Mountains	332	97	14.0	1.1	SA
28	Kermanshah	Zagros Mountains	446	119	14.5	1.0	SA
29	Khorramabad	Zagros Mountains	502	128	17.2	1.1	SA
30	Sanandaj	Zagros Mountains	438	120	13.7	1.1	SA
31	Shahrekord	Zagros Mountains	324	92	11.6	0.8	SA

All the above indices are averaged over the last 60-year period from 1960 to 2019. Furthermore, SD denotes standard deviation.

2.2. Methodology

2.2.1. Data quality test

The quality of each synoptic station's data is assured by IRIMO before being presented to users. Suspicious data are strictly checked out and subjected to WMO procedures before use (Balling et al. 2016; Shirvani 2015; WMO 2003). In this regard, Grubbs test (Grubbs and Beck 1972) was applied to identify outlier data point. In this procedure, when one or more data points in one station was detected as an outlier, the data points at the same year from one or more neighbour stations had to be investigated. If these data points did not match the outlier, the outlier was identified for sure and removed from the time series; otherwise, it is considered as a valid data point. This test was applied to all the data in this study.

2.2.2. Modified De Martonne aridity index

An aridity index is a numerical indicator of the degree of dryness in the climate at a selected location. In this study, we used the modified De Martonne aridity index (I_{DM}) to classify the climate conditions in eight classes, from hyper-arid to hyper-humid (Table 2). I_{DM} is based on the ratios of precipitation and air temperature and defined as the following equation (De Martonne 1926; Zarei et al. 2019):

$$I_{DM} = \frac{P_{mean}}{T_{mean} + 10}$$

$$(1)$$

where

P_{mean} is average of precipitation (mm)

T_{mean} is average of air temperature (°C)

I_{DM} is Modified De Martonne aridity index

Table 2
Climatic classification of Modified De Martonne
aridity index (De Martonne 1926; Zarei et al. 2019)

Symbol	Climate condition	Index range
HA	Hyper-arid	$I_{DM} < 5$
A	Arid	$5 \leq I_{DM} < 10$
SA	Semi-arid	$10 \leq I_{DM} < 20$
M	Mediterranean	$20 \leq I_{DM} < 24$
SH	Sub-humid	$24 \leq I_{DM} < 28$
H	Humid	$28 \leq I_{DM} < 35$
HHA	Hyper-humid type A	$35 \leq I_{DM} < 55$
HHB	Hyper-humid type B	$55 \leq I_{DM}$

2.2.3. Time series monotonic analysis

We analysed time series of interest by (i) Mann-Kendall test for trend analysis, (ii) Sen's slope estimator for calculating magnitude of the trend line, and (iii) Pettitt test for detecting abrupt changes in time series.

The Mann-Kendall (M-K) trend test (Kendall 1975; Mann 1945) is a rank-based non-parametric test in determining statistically significant trend in a time series. The correlation between the rank order of the observed values and their chronological order are considered in this test. We herein carried out the M-K trend test in each station at $\alpha = 0.05$, $\alpha = 0.01$, and $\alpha = 0.001$ significance levels, and identified increasing or decreasing monotonic trends at 95%, 99%, and 99.9% confidence intervals, respectively.

It is important to note that positive serial correlation in a time series tends to increase the chance of being significant in the M-K test. In other words, when serial correlation in data is significant, the positive or negative serial correlation will alter *Var (S)* value to be less or more than real value. Hamed and Rao (1998) proposed the modified M-K trend test to remove the effects of serial correlation. The details of the method can be found elsewhere e.g. (Daneshvar Vousoughi et al. 2013; Dinpashoh et al. 2011; Jhajharia et al. 2014; Partal and Kahya 2006).

Sen's slope estimator

Sen's slope estimator (Sen 1968) is a non-parametric linear regression slope that is a better alternative to simple linear regression. In this method, the effects of outlier data points on the results of the trend are negligible which can be considered as the major advantage over other parametric methods. The details of the method can be found elsewhere e.g. (Daneshvar Vousoughi et al. 2013; Dinpashoh et al. 2011; Jhajharia et al. 2014; Partal and Kahya 2006) .

The Pettitt test (Pettitt 1979) was utilized in identifying potential abrupt changes in a time series for each of the considered indices and calculates their statistical significance (Bickici Arikan and Kahya 2019). This test is non-parametric rank-based and distribution-free so that it is insensitive to outliers. In this study, we performed this test at 95% and 99% confidence intervals (α = 0.05, and α = 0.01) for detecting abrupt change. Aftermath the average amount of changes can be calculated for post-breakpoint against pre-breakpoint. Trends for pre- and post-breakpoint series were obtained using simple linear regression (performed only for series with a significant Pettitt test at the 0.01 level). One of our innovations in this research study was using the Pettitt test for detection of multiple abrupt changes in the time series. For those series that had one significant breakpoint (at a 0.01 level), the time series was divided into two sub-series at the detected point. Then the Pettitt test was applied again for the both sub-series. This is repeated if there were a significant change point in any sub-series.

2.2.4. Spatial analysis

Cokriging geostatistical technique was employed for the interpolation of the analysis indices over Iran using 96 stations to extract high resolution maps for the period 2009–2018. The details of the method can be found elsewhere e.g. (Rostami et al. 2020; Yang et al. 2021)

2.2.5. Return periods

Return periods can be used to develop plans and policies for reducing risk and loss caused by extreme climate events in both short and long-term planning. Using EasyFit5.5 software, we performed a comprehensive frequency analysis considering 65 different distributions and determined then the best-fit probability distribution through the Kolmogorov-Smirnov test at each station. Through the cumulative distribution of the selected probability distribution, we computed magnitudes of the variable under consideration with respect to the following return periods: 2-, 10-, 25-, 50-, and 100-year. This was repeated for each climate variable in the rest of analysis.

3. Results And Discussion

It is evident in Fig. 2 that the highest differences between T_{min} and T_{max} changes were observed in the eastern and southeastern Iran as well as at the stations located in the Zagros mountain range whereas the lowest differences were found in the coastal area in the Caspian Sea.

3.1. Trend analysis

An overall evaluation of the results given Table 3 and Fig. 3 points out that 50% of the stations had a significant decreasing FD trend (at the 0.05 level). In fact, global warming has led to significant reduction in frost days in half of all the stations over the past 60 years. The lowest trend slope was observed in the northeast, in which FD decreased approximately 6 days per decade. Nevertheless, 10% of stations have also experienced a significant increasing trend in their FD time series, whereby FD has risen up 6 days per decade in Shahrekord. Similar indication was documented earlier by Caloiero (2017) who found positive FD trends in some parts of New Zealand. In general, global warming is expected to cause decrease in FD; however, we discovered opposite conditions so that FD trend has been increasing or close to zero at some stations mostly located in cold and mountainous regions. Along the coastal areas in the Caspian Sea, FD has dramatically reduced; however, conflicting results with other stations were observed in Gorgan, which is located in the eastern side of the Caspian Sea and has a drier climate than the rest of the coastal area. It is worthwhile to mention that no frost days have been recorded in Bandarabbas in the last 60 years. It is located in one of the most tropical parts of Iran, so that annual T_{mean} of that station was calculated as 27 ºC being the highest value among all the stations. The results of Shi et al. (2018) showed that frost days decreased with a slope of 2.9 days per decade in China during the period 1961–2015. Our findings similarly indicated that frost days were decreased 2 days per decade on average during the last 60 years in Iran.

Table 3 Magnitude of Sen's slope estimator. Significance levels are shown using M-K test with the background colour

No.	Station name	Frost days	Tmin (ºC)	Tmax (ºC)	Tmean (ºC)	Tminmin (ºC)	Tmaxmax (ºC)	Tsoil-min (ºC)	IDM	Precipitation (mm)
1	Esfahan	-0.08	0.03	0.03	0.03	0.02	0.03	-0.05	0.02	0.78
2	Kerman	-0.46	0.05	0.03	0.04	0.06	0.03	0.01	-0.04	-0.78
3	Shiraz	-0.33	0.05	0.03	0.04	0.02	0.02	-0.02	-0.02	-0.15
4	Yazd	-0.70	0.08	0.02	0.05	0.10	0.01	0.09	-0.01	-0.11
5	Anzali	-0.08	0.04	0.00	0.02	0.03	0.00	0.01	-0.10	-0.92
6	Babolsar	-0.13	0.05	0.02	0.03	0.06	0.03	0.02	0.02	1.81
7	Gorgan	0.22	-0.01	0.03	0.01	-0.02	0.02	-0.03	-0.12	-3.26
8	Ramsar	-0.17	0.05	0.02	0.03	0.04	0.05	0.03	-0.07	-0.32
9	Rasht	-0.39	0.04	0.01	0.03	0.06	0.02	0.02	-0.06	-0.51
10	Bandarabbas	-	0.01	0.01	0.01	-0.04	0.03	-0.02	0.00	0.04
11	Bushehr	0.00	0.05	0.02	0.04	0.03	0.00	0.00	0.02	0.86
12	Birjand	0.09	0.00	0.01	0.00	-0.06	0.00	-0.02	-0.03	-0.79
13	Abadan	0.00	0.05	0.04	0.04	0.02	0.04	0.02	0.00	0.28
14	Ahvaz	0.00	0.07	0.03	0.05	0.04	0.02	-0.01	-0.02	-0.28
15	Mashhad	-0.88	0.08	0.03	0.06	0.17	0.04	0.02	-0.03	0.03
16	Sabzevar	-0.75	0.07	0.03	0.05	0.11	0.01	0.02	0.00	0.19
17	Torbat H.	-0.09	0.03	-0.01	0.01	0.07	-0.02	0.00	-0.03	-0.71
18	Khoy	-0.13	0.05	0.04	0.04	-0.01	0.03	0.01	-0.06	-0.87
19	Orumiyeh	0.38	0.01	0.03	0.02	0.02	0.01	-0.02	-0.04	-0.78
20	Tabriz	0.09	0.04	0.04	0.04	0.06	0.01	-0.03	-0.09	-1.53
21	Zanjan	-0.35	0.03	0.02	0.03	0.07	0.02	-0.02	-0.05	-0.65
22	Bam	-0.15	0.06	0.03	0.05	0.06	0.03	0.02	-0.01	-0.09
23	Zahedan	-0.36	0.04	0.02	0.03	0.04	0.01	-0.03	-0.02	-0.50
24	Qazvin	0.00	0.02	0.02	0.02	0.03	0.02	-0.03	0.00	0.35
25	Shahrud	-0.45	0.06	0.01	0.03	0.07	0.02	0.04	-0.01	-0.12
26	Tehran	-0.73	0.06	0.02	0.04	0.07	0.01	0.01	0.01	0.46
27	Arak	0.22	0.02	0.01	0.02	0.07	0.01	-0.02	-0.08	-1.69
28	Kermanshah	-0.32	0.05	0.04	0.05	0.08	0.01	-0.04	-0.10	-1.75
29	Khorramabad	0.52	-0.02	0.00	-0.01	-0.02	0.00	-0.03	-0.03	-1.27
30	Sanandaj	-0.36	0.03	0.05	0.04	0.10	0.03	0.00	-0.15	-2.66
31	Shahrekord	0.63	-0.03	0.00	-0.02	0.00	-0.03	-0.09	-0.01	-0.37

Significant positive trend at 0.001	Significant positive trend at 0.01	Significant positive trend at 0.05	Insignificant positive trend	Insignificant negative trend	Significant negative trend at 0.05	Significant negative trend at 0.01	Significant negative trend at 0.001

The analysis of T_{min} (T_{max}) time series revealed that 71% (68%) of all the stations had a significant positive trend at the 0.05 level. The Shahrekord station, which has the most elevated location with an altitude of more than 2000 meters, showed contrasting results to other stations in such a way that T_{min}

demonstrated statistically significant negative trend. Some stations have experienced fairly strong increasing trends as the both T_{min} and T_{max} trends were significant at 61% and 48% of the stations at the 0.001 level, respectively. One of our striking findings in this study is that the increase in T_{min} values was sharper than in T_{max} values. Although many researchers have acknowledged this fact, some opposite results have been also reported (e.g., Caloiero (2017) for New Zealand). Wang et al. (2018b) stated that T_{min} contributed greatly to the overall T_{mean} increases in northern China. They have claimed that warm air temperature indices appeared to be increasing since late 1980s and early 1990s. Our results concerning the increase in T_{max}, which was often started during the mentioned period in Iran, confirmed their indications. In addition, Yosef et al. (2019) concluded similar results in Israel.

The results of T_{mean} showed that the stations located in the Zagros mountainous regions are less warmer than other regions so that the Shahrekord station has even experienced significant negative trend. Moreover, Shirvani (2015) came to similar conclusion that a decreasing trend was one of characteristic behaviours in the T_{mean} time series at Shahrekord. His findings also demonstrated that the increasing trend of T_{mean} was sharper in the southwest of the country. Pokorná et al. (2018) presented that the surface air temperature trends are not geographically monotonous in different regions of the world. Anyhow, the picture in this study has been consistent with the common expectation that T_{mean} has risen up 0.3 °C per decade on average over the past 60 years in Iran, indicating that the increase in air temperature in Iran was higher than the global average. In a recent study conducted in Iraq (Iran's western neighbour), Salman et al. (2017) suggested that air temperature in the country had been increasing 2 to 7 times faster than global mean surface air temperature rise.

In the case of T_{minmin} analysis, our results showed that 65% of all the stations experienced a significant positive trend while 6% of the stations had a significant negative trend at the 0.05 level. The increase in T_{minmin} in the northeastern part of the country was so sharp that the slope of trend based on the Sen's method occurred as an increase of 1.2 °C per decade. A similar pattern appeared in its counterpart variable so that significant positive trends in T_{maxmax} values were observed in 55% of stations.

In the case of the soil related temperature variable, the analysis of $T_{soil-min}$ time series revealed that almost half of all the stations had increasing trends whereas the remaining half had decreasing trends. Out of all the stations, we detected significant positive trends in 19% stations as well as significant negative trends in another 19% of the stations at the 0.05 level. Our findings also revealed that no station has been noted to have an increasing $T_{soil-min}$ trend in the Zagros Mountains. Most of the stations located in the northwest part of the country, where similar geologic conditions alike the Zagros Mountains exist, have also demonstrated a declining behaviour in $T_{soil-min}$ values, but none of them have been statistically significant. Qian et al. (2011) reported that, a significant negative trend was observed for T_{soil} in eastern Canada. Furthermore, the increasing trend of $T_{soil-min}$ was observed in the northeastern stations of Iran as well as in the stations located in the coastal regions of the Caspian Sea (except the Gorgan station). In a recent study focusing on the north eastern Iran for the period 1993–2016, Araghi et al.

(2017) showed that trend of soil surface temperature was positive in warmer months while negative in colder months. We also found that mean annual $T_{soil-min}$ and mean annual T_{min} differently behaved and this distinction between the two varies between – 1.2 ºC to -3.5 ºC in various locations in Iran. This feature could be interpreted by precipitation changes and snow cover as well as solar radiation and other meteorological indices such as humidity and wind speed. Zhang et al. (2005) has obtained similar results for Canada.

In a summary presented in Fig. 3 and Table 3, about 75% of all the stations have exhibited negative trends (p > 0.05) or such tendencies in the I_{DM} aridity index and total annual precipitation. More specifically, nearly 20% of all the stations showed a statistically significant negative trend in both precipitation and I_{DM} values (p < 0.05). A negative trend in precipitation was previously reported in some regions of Iran by Dinpashoh et al. (2014) and Zamani et al. (2017). Şarlak and Mahmood Agha (2018) has also reported a sharp declining trend in I_{DM} aridity index in Iraq. In the Zagros mountain ranges and the northwestern regions, the rainfall showed declining trend in all stations and its average value was decreased by an average rate of 15 and 10 mm per decade, respectively. The east of the Caspian Sea (Gorgan) and Zagros mountainous region has become drier more than all other areas. In the east of the Caspian Sea, the increase in air temperature was not statistically significant; therefore, the significant decrease of rainfall was thought to be the main reason for the dramatic decrease in I_{DM} aridity index in the area. In general, the increasing air temperature on one side and declining precipitation on the other side have caused a noticeable decrease in the I_{DM} aridity index in Iran. The results of Tabari et al. (2014), Gholami et al. (2017) and Mianabadi et al. (2019) are consistent with the findings of this study regarding decreasing trends in the I_{DM} aridity index in Iran.

3.2. Change point detection

The results illustrated in Fig. 3 and Fig. 4 show that an abrupt upward change, which was mostly observed in the 1990s, occurred at the 90% of all the T_{mean} time series. In more detail, most of T_{min} and T_{max} change points detected in the first and second half of the decade of 1990, respectively. Abrupt changes of I_{DM} and precipitation were also downward in 26% of all the stations. It seems that abrupt downward changes in the I_{DM} series in the western and northwestern Iran were greater than those in other regions. It is important to emphasize that the areas in the eastern parts of the country (i.e., Kerman and Birjand) were categorized as arid areas before I_{DM} abrupt downward change; however, after the shift in 1997, they have transformed to hyper-arid areas. Abrupt downward changes in the eastern Caspian Sea (Gorgan) and a station in the Zagros mountain range (Sanandaj) have also caused these areas to change their phase from Mediterranean to semi-arid.

As shown in Fig. 4, 60% of the stations revealed an abrupt downward change in FD mostly during the 1990s. Nevertheless, 20% of the stations experienced an abrupt upward change mainly during the 1980s or 1970s, but none occurred during the 1990s. It is important to note that no significant increasing air temperature trend was observed in all the stations experiencing an abrupt upward change in their FD time series. The highest decrease in FD was observed in Mashhad, located in the northeastern Iran, where the

mean value of FD reduced about 30 days after the shift. The pattern of $T_{soil-min}$ changes seemed to be contradictory to the other temperature indices, since it had an abrupt downward change at 50% of all the stations that mostly occurred in the 1980s whereas it had opposite change at 30% of all the stations.

3.3. Time series trends before and after the abrupt change

Four patterns are distinguishable in the trend patterns of our data set. For the sake of brevity, our demonstration charts are limited to six of the selected stations in each type. The first type includes the stations that experienced a decreasing trend pre- and post-breakpoint series (Fig. 5a). In contrast to the first one, the second type corresponds to the stations that had an increasing trend in pre- and post-breakpoint series (Fig. 5b). The third type is dedicated to the stations that, the negative trend turned to positive due to the shift in such a way that the series contains a declining (increasing) trend before (after) the breakpoint (Fig. 5c). The fourth type is opposite to the third; that is to say, the series experiences an increasing trend before breakpoint and decreasing afterwards (Fig. 5d). Our analysis revealed that FD trends belonging to Type 1 were noted in 40% of the stations in the form of decreasing pre- and post-breakpoint. In nearly 30% of the stations, FD trends followed Type 4 in the form of increasing before breakpoint and decreasing afterwards.

Analysis of T_{min} time series revealed that the trends occurred as increasing before and after the breakpoint in the majority of the stations. In some stations mostly located in the cold and mountainous regions, the trend in T_{min} series was negative before the shift and positive afterwards. Unlike T_{min} series, a considerable number of stations followed Type 3 pattern regarding T_{max}. At the majority of all the stations located in the northwest parts of the country where cold and mountainous areas take place, the trend in T_{mean} series was decreasing before the change point and increasing afterwards (Type 3), while the trend was positive over the entire period (Type 2) in the central, southeastern and northeastern regions of Iran. In the same context, the results of Reeves et al. (2007) showed that the trend in the annual T_{mean} time series was decreasing during the 1960–1985 period in Libby, Montana in the United States, but an abrupt upward change caused the series to have increasing trends. Moreover, Fioravanti et al. (2016) presented similar results for Italy. In this study, we found that the trends in T_{minmin} and T_{maxmax} series after change point were increasing in more than 70% of the stations. A careful look on the $T_{soil-min}$ results showed that the trend was increasing after the breakpoint in the majority of the stations that experienced an abrupt shift at the 0.01 significance level.

About half of the stations had an abrupt downward change and their $T_{soil-min}$ values before the shift were higher than the latter values; therefore, the resulted overall trend in these stations was decreasing. In these stations, the trend in $T_{soil-min}$ was rising after the breakpoint in accordance with other temperature indices due to global warming; but the reason behind why most of these stations experienced an abrupt downward change in the 1980s can have various causes which will be addressed later. In a relevant study, Wang et al. (2018a) reported that increasing trend of $T_{soil-min}$ in China is at least doubled since 1998.

For I_{DM} and precipitation time series, Gorgan (located in the east of the Caspian Sea) is a good example; the trend of precipitation in this station was increasing at a rate of 24 mm per decade until 1982, but an abrupt downward change led to a decreasing trend in the series at a rate of 10 mm per decade after the change point. Since 1982, decreasing precipitation along with temperature growth at a rate of 0.3 °C per decade at this station has led to a reduction in I_{DM} at a rate of 0.5 per decade, while I_{DM} was increasing at a rate of 0.2 per decade before the change point. In other words, the climate conditions in Gorgan used to be humid at a low rate, but after an abrupt shift that occurred in 1982, it started to be drier. Therefore, we can speculate that the aridity conditions in this region has been shifting from Mediterranean to semi-arid due to global warming and climate change.

3.4. Multiple abrupt changes in time series

Over a long period of time, climatic patterns can possibly shift multiple times (Yu and Ruggieri (2019). To provide a better analysis of the results, five types were defined as below:

(i) Time series that experienced two abrupt upward changes is categorized as Type 1 (Fig. 6a). (ii) Type 2 is defined as the time series having two abrupt downward changes (Fig. 6b). (iii) Type 3 presents time series that experienced an initial abrupt change in upward direction and downward afterwards (Fig. 6c). (iv) Type 4 represents the time series in which the first abrupt change was downward as the second one was upward (Fig. 6d). Finally, (v) Type 5 is defined as the time series containing three abrupt changes (Fig. 6e). The indices of I_{DM}, precipitation and T_{maxmax} did not have more than one abrupt shift in their time series in any station. In the case of T_{min} time series, 14 stations were identified to have two abrupt upward changes. Four stations (Ahvaz, Bushehr, Kermanshah, and Yazd) mostly located in the tropical regions experienced three abrupt upward changes in T_{min} time series. The Modified Pettitt test analysis for T_{max} revealed that multiple abrupt changes were observed only in five stations, while in all of them, the first abrupt shift was downward and the second one was upward (Type 4). In addition, Reeves et al. (2007) showed that the annual T_{mean} time series in Libby, Montana in the United States experienced two change points between 1960 and 2000, so that the first abrupt change was downward and the second one was upward. In most stations, two abrupt upward changes were detected in T_{mean} time series, and the second change point occurred in a shorter time interval than the first change point.

As previously discussed, some of the studied indices (especially T_{max}) had an abrupt downward change and a decreasing trend between 1970 and 1980 in some stations. A detailed review in earlier studies revealed that results of Easterling et al. (1997) are consistent with the outcomes of our research concerning T_{max} in the southeastern Asia. Moreover, Yu and Ruggieri (2019) claimed that global surface temperature experienced an abrupt downward change between 1963 and 1976. They explained that the cause of this event could be World War I and II (1914–1918 and 1939–1945), particularly the Great Depression (1929–1933) and other recessions (such as 1938, 1945 and 1958) that subsequently induced a reduction to greenhouse gas emissions due to the downfall of economic activities and closure of many factories. Greenhouse gas molecules remain in the atmosphere for decades, so the planet's temperature may not respond until the greenhouse gases begin to dissipate. In another relevant study, Pokorná et al.

(2018) demonstrated that global warming has never been ubiquitous so that here are seasons, regions and time periods with negligible or even negative air temperature trends (frequently referred to as warming holes). Therefore, we speculate that the abrupt downward change in T_{max} or negative trend in $T_{soil-min}$ in some stations might be occurred due to aforementioned causes.

3.5. Return period

After a consecutive analysis procedure applied for the calculation of return periods in each of 31 stations, the magnitudes with respect to the five return periods at 9 selected stations are plotted in Fig. 7. It is evident that the highest increases in FD return periods' values were frequently observed at the stations located in the coastal area across the Caspian Sea. Due to limited space, we can only briefly refer here to the highlights of our return period computations of all the stations. The highest magnitudes of T_{mean} with respect to the return periods under consideration (i.e. 10-, 25-, 50- and 100-year) were observed in the northwest region of Iran. In particular, increase (hereafter defined as a deviation from the average value of the study period) in T_{mean} at Khoy and Zanjan stations appeared to be highest among 31 stations for all the return periods; for example, it valued as 3.1°C (approximately %25) for the 100-year. A group of 5 stations in the northwest region including these two stations exhibited a value of 2.7 °C as the mean increase in magnitude for the 100-year return period.

A group of 7 stations in the west and northwest region deviated from the rest of stations by having high increase value in $T_{soil-min}$ for all the return periods. As noted in T_{mean} case, highest increases in $T_{soil-min}$ among all stations for the 100-year return period were computed with a value of 4.1, 4.5 and 4.9°C at Khoy, Khorramabad and Zanjan stations, respectively. The mean increase in magnitude of this group is 3.96 °C for the 100-year return period. For the case rainfall, Yazd, Bandarabbas and Bushehr stations, which are located in a hyper-arid area having high decrease amount in I_{DM}, exhibited highest increases in rainfall for all the return periods. This case might refer to a flooding potential in these areas. The lowest magnitudes of T_{minmin} with respect to the 50- and 100-year return periods was computed as -37.9 °C and – 35.0 °C at Shahrekord station, respectively. The highest values of T_{maxmax} with respect to the 100-year return period were found in Abadan and Ahvaz stations (located in the southwest of the country) having a respective magnitude of 53.1 °C and 52.9 °C.

4. Conclusions

In general, the temperature has increased with less intensity in the cold regions in comparison to the tropical regions. A coupled effect of increased air temperature and diminished rainfall have resulted in decrease in I_{DM} aridity index by 0.35 per decade on the average across the country. The Zagros mountainous region has exhibited drier conditions than other areas as its I_{DM} decreased at a rate of 0.7 per decade on the average. Similarly, the northwest Iran has become drier due to reduced rainfall and increased air temperature. It is noteworthy to mention that Gorgan has noticeably dried up having significant decrease in rainfall amounts as the rate of rainfall reduction in Gorgan reached 33 mm per decade. An abrupt upward change in T_{mean} series, in which most of these change points occurred during

the 1990s was detected in more than 90% of the stations. A modified Pettitt test was utilized to determine multiple change points. Our results showed that, four stations located mainly in the tropical regions of the country experienced three abrupt upward changes in the T_{min} time series. The results of $T_{soil-min}$ showed that about half of all the stations had negative trend, that is opposite to the behaviors of the other temperature indices. However, it is evident that the trend in the $T_{soil-min}$ series was positive after the change point in most stations with an abrupt shift. In other words, the $T_{soil-min}$ trends have been positive or close to zero at 90% of the stations since 1985.

In general, we herein speculate that global warming has caused Iran to have warmer and drier climate with more extreme air temperature conditions. As long as the policy of sustainable control of greenhouse gas emissions remains excluded from the agenda of all countries around the world, temperature related increasing trends due to global warming will keep growing at a higher intensity. One of the most effective ways to prevent this crisis is to take advantage of using renewable energy instead of fossil fuels. As an alternative solution, Gorjian et al. (2019) indicated that Iran has a high potential in solar energy as the annual rate of solar energy in Iran is estimated at a range of 4.5–5.5 kWh/m^2. The outcomes of our study can be useful in revealing the impacts of global warming and climatic change as well as providing a more comprehensive viewpoint for continuing researchers on the subject.

Declarations

Declaration of Competing Interest

Funding information

CRediT authorship contribution statement

Amin Sadeqi: Conceptualization, Data curation, Formal analysis, Investigation, Methodology, Preparation, Resources, Software, Visualization, Funding acquisition, Writing - original draft.

Ercan Kahya: Data curation, Supervision, Formal analysis, Validation, Writing - Review & Editing.

Availability of data and material

Data used in the present study are available on the website of Iran Meteorological Organization, IRIMO (https://data.irimo.ir/).

Consent for publication

Informed consent to publish has been obtained from each participant.

Consent to participate

All authors give their consent for participate of this paper.

Acknowledgements

Code availability and Ethics approval

Not applicable.

References

Araghi A, Mousavi-Baygi M, Adamowski J (2017) Detecting soil temperature trends in Northeast Iran from 1993 to 2016. Soil Tillage Res 174:177–192 https://doi.org/10.1016/j.still.2017.07.010

Asseng S et al. (2014) Rising temperatures reduce global wheat production. Nat Clim Change 5:143–147 https://doi.org/10.1038/nclimate2470

Balling RC, Kiany MSK, Roy SS (2016) Anthropogenic signals in Iranian extreme temperature indices. Atmos Res 169:96–101 https://doi.org/10.1016/j.atmosres.2015.09.030

Bickici Arikan B, Kahya E (2019) Homogeneity revisited: analysis of updated precipitation series in Turkey. Theor Appl Climatol 135:211–220 https://doi.org/10.1007/s00704-018-2368-x

Caloiero T (2017) Trend of monthly temperature and daily extreme temperature during 1951–2012 in New Zealand. Theor Appl Climatol 129:111–127 https://doi.org/10.1007/s00704-016-1764-3

Daneshvar Vousoughi F, Dinpashoh Y, Aalami MT, Jhajharia D (2013) Trend analysis of groundwater using non-parametric methods (case study: Ardabil plain). Stochastic Environ Res Risk Assess 27:547–559 https://doi.org/10.1007/s00477-012-0599-4

De Martonne E (1926) Aréisme et indice d'aridité. Comptes Rendus de L'Academy of Science, Paris 182:1395-1398

Dezfuli AK, Karamouz M, Araghinejad S (2010) On the relationship of regional meteorological drought with SOI and NAO over southwest Iran. Theor Appl Climatol 100:57–66 https://doi.org/10.1007/s00704-009-0157-2

Dinpashoh Y, Jhajharia D, Fakheri-Fard A, Singh VP, Kahya E (2011) Trends in reference crop evapotranspiration over Iran. J Hydrol 399:422–433 https://doi.org/10.1016/j.jhydrol.2011.01.021

Dinpashoh Y, Mirabbasi R, Jhajharia D, Abianeh HZ, Mostafaeipour A (2014) Effect of Short-Term and Long-Term Persistence on Identification of Temporal Trends. J Hydrol Eng 19:617–625 https://doi.org/10.1061/(ASCE)HE.1943-5584.0000819

Easterling DR et al. (1997) Maximum and Minimum Temperature Trends for the Globe. Science 277:364–367 https://doi.org/10.1126/science.277.5324.364

Estrada F, Botzen WJW, Tol RSJ (2017) A global economic assessment of city policies to reduce climate change impacts. Nat Clim Change 7:403–406 https://doi.org/10.1038/nclimate3301

Fioravanti G, Piervitali E, Desiato F (2016) Recent changes of temperature extremes over Italy: an index-based analysis. Theor Appl Climatol 123:473–486 https://doi.org/10.1007/s00704-014-1362-1

Gebrechorkos SH, Hülsmann S, Bernhofer C (2019) Long-term trends in rainfall and temperature using high-resolution climate datasets in East Africa. Sci Rep 9:1–9 https://doi.org/10.1038/s41598-019-47933-8

Gholami V, Ahmadi Jolandan M, Torkaman J (2017) Evaluation of climate change in northern Iran during the last four centuries by using dendroclimatology. Nat Hazards 85:1835–1850 https://doi.org/10.1007/s11069-016-2667-4

Gorjian S, Zadeh BN, Eltrop L, Shamshiri RR, Amanlou Y (2019) Solar photovoltaic power generation in Iran: Development, policies, and barriers. Renewable Sustainable Energy Rev 106:110–123 https://doi.org/10.1016/j.rser.2019.02.025

Grubbs FE, Beck G (1972) Extension of Sample Sizes and Percentage Points for Significance Tests of Outlying Observations. Technometrics 14:847–854 https://doi.org/10.1080/00401706.1972.10488981

Hamed KH, Rao AR (1998) A modified Mann-Kendall trend test for autocorrelated data. J Hydrol 204:182–196 https://doi.org/10.1016/S0022-1694(97)00125-X

IPCC (2013) Climate Change 2013: The Physical Science Basis, Contribution of Working Group I to the Fifth Assessment Report of the Intergovernmental Panel on Climate Change. Cambridge University Press. https://www.ipcc.ch/report/ar5/wg1/

IPCC (2014) Climate Change 2014: Mitigation of climate change, Contribution of Working Group III to the Fifth Assessment Report of the Intergovernmental Panel on Climate Change. Cambridge University Press. https://www.ipcc.ch/report/ar5/wg3/

Jhajharia D, Dinpashoh Y, Kahya E, Choudhary RR, Singh VP (2014) Trends in temperature over Godavari River basin in Southern Peninsular India. Int J Climatol 34:1369–1384 https://doi.org/10.1002/joc.3761

Kahya E (2011) The Impacts of NAO on the Hydrology of the Eastern Mediterranean. In: Hydrological, Socioeconomic and Ecological Impacts of the North Atlantic Oscillation in the Mediterranean Region. Springer, Dordrecht, The Netherlands, pp 57–71. https://doi.org/10.1007/978-94-007-1372-7_5

Kendall MG (1975) Rank correlation methods. Charles Griffin, London.,

Labat D, Goddéris Y, Probst JL, Guyot JL (2004) Evidence for global runoff increase related to climate warming. Adv Water Resour 27:631-642 https://doi.org/10.1016/j.advwatres.2004.02.020

Lenton TM, Dakos V, Bathiany S, Scheffer M (2017) Observed trends in the magnitude and persistence of monthly temperature variability. Sci Rep 7:1–10 https://doi.org/10.1038/s41598-017-06382-x

Mann HB (1945) Nonparametric tests against trend. Econometrica: Journal of the Econometric Society 13:245–259 https://doi.org/10.2307/1907187

Mianabadi A, Shirazi P, Ghahraman B, Coenders-Gerrits AMJ, Alizadeh A, Davary K (2019) Assessment of short- and long-term memory in trends of major climatic variables over Iran: 1966–2015. Theor Appl Climatol 135:677–691 https://doi.org/10.1007/s00704-018-2410-z

Mostafa AN et al. (2019) Past (1950–2017) and future (–2100) temperature and precipitation trends in Egypt. Weather Clim Extremes 26:100225 https://doi.org/10.1016/j.wace.2019.100225

Partal T, Kahya E (2006) Trend analysis in Turkish precipitation data. Hydrol Processes 20:2011–2026 https://doi.org/10.1002/hyp.5993

Pettitt AN (1979) A non-parametric approach to the change-point problem. J R Stat Soc C-Appl 28:126–135 https://doi.org/10.2307/2346729

Pokorná L, Kučerová M, Huth R (2018) Annual cycle of temperature trends in Europe, 1961–2000. Global and Planet Change 170:146–162 https://doi.org/10.1016/j.gloplacha.2018.08.015

Qian B, Gregorich EG, Gameda S, Hopkins DW, Wang XL (2011) Observed soil temperature trends associated with climate change in Canada. J Geophys Res Atmos 116 https://doi.org/10.1029/2010JD015012

Reeves J, Chen J, Wang XL, Lund R, Lu QQ (2007) A Review and Comparison of Changepoint Detection Techniques for Climate Data. J Appl Meteor Climatol 46:900–915 https://doi.org/10.1175/JAM2493.1

Rostami AA, Karimi V, Khatibi R, Pradhan B (2020) An investigation into seasonal variations of groundwater nitrate by spatial modelling strategies at two levels by kriging and co-kriging models. J Environ Manage 270:110843 https://doi.org/10.1016/j.jenvman.2020.110843

Salman SA, Shahid S, Ismail T, Chung E-S, Al-Abadi AM (2017) Long-term trends in daily temperature extremes in Iraq. Atmos Res 198:97–107 https://doi.org/10.1016/j.atmosres.2017.08.011

Salzmann M (2016) Global warming without global mean precipitation increase? Sci Adv 2:e1501572 https://doi.org/10.1126/sciadv.1501572

Şarlak N, Mahmood Agha OMA (2018) Spatial and temporal variations of aridity indices in Iraq. Theor Appl Climatol 133:89–99 https://doi.org/10.1007/s00704-017-2163-0

Sen PK (1968) Estimates of the Regression Coefficient Based on Kendall's Tau. J Am Stat Assoc 63:1379–1389 https://doi.org/10.1080/01621459.1968.10480934

Shi J, Cui L, Ma Y, Du H, Wen K (2018) Trends in temperature extremes and their association with circulation patterns in China during 1961–2015. Atmos Res 212:259–272 https://doi.org/10.1016/j.atmosres.2018.05.024

Shirvani A (2015) Change point analysis of mean annual air temperature in Iran. Atmos Res 160:91–98 https://doi.org/10.1016/j.atmosres.2015.03.007

Sinha J, Das J, Jha S, Goyal MK (2020) Analysing model disparity in diagnosing the climatic and human stresses on runoff variability over India. J Hydrol 581:124407 https://doi.org/10.1016/j.jhydrol.2019.124407

Tabari H, Hosseinzadeh Talaee P, Mousavi Nadoushani SS, Willems P, Marchetto A (2014) A survey of temperature and precipitation based aridity indices in Iran. Quaternary International 345:158–166 https://doi.org/10.1016/j.quaint.2014.03.061

van Oldenborgh GJ et al. (2009) Western Europe is warming much faster than expected. Clim Past 5:1–12 https://doi.org/10.5194/cp-5-1-2009

Vazifehkhah S, Kahya E (2018) Hydrological drought associations with extreme phases of the North Atlantic and Arctic Oscillations over Turkey and northern Iran. Int J Climatol 38:4459–4475 https://doi.org/10.1002/joc.5680

Vazifehkhah S, Kahya E (2019) Hydrological and agricultural droughts assessment in a semi-arid basin: Inspecting the teleconnections of climate indices on a catchment scale. Agric Water Manage 217:413–425 https://doi.org/10.1016/j.agwat.2019.02.034

Vazifehkhah S, Tosunoglu F, Kahya E (2019) Bivariate Risk Analysis of Droughts Using a Nonparametric Multivariate Standardized Drought Index and Copulas. J Hydrol Eng 24:05019006 https://doi.org/10.1061/(ASCE)HE.1943-5584.0001775

Wang L, Henderson M, Liu B, Shen X, Chen X, Lian L, Zhou D (2018a) Maximum and Minimum Soil Surface Temperature Trends Over China, 1965–2014. J Geophys Res Atmos 123:2004–2016 https://doi.org/10.1002/2017JD027283

Wang X et al. (2018b) Temporal and spatial variation of extreme temperatures in an agro-pastoral ecotone of northern China from 1960 to 2016. Sci Rep 8:1–14 https://doi.org/10.1038/s41598-018-27066-0

WMO (2003) Guidelines on Climate Metadata and Homogenization. WMO/TD-No. World Meteorological Organization, Geneva http://refhub.elsevier.com/S0169-8095(15)00311-7/rf0185

Yang B et al. (2021) Spatio-temporal Cokriging method for assimilating and downscaling multi-scale remote sensing data. Remote Sens Environ 255:112190 https://doi.org/10.1016/j.rse.2020.112190

Yosef Y, Aguilar E, Alpert P (2019) Changes in extreme temperature and precipitation indices: Using an innovative daily homogenized database in Israel. Int J Climatol 39:5022–5045 https://doi.org/10.1002/joc.6125

Yu M, Ruggieri E (2019) Change point analysis of global temperature records. Int J Climatol 39:3679–3688 https://doi.org/10.1002/joc.6042

Zamani R, Mirabbasi R, Abdollahi S, Jhajharia D (2017) Streamflow trend analysis by considering autocorrelation structure, long-term persistence, and Hurst coefficient in a semi-arid region of Iran. Theor Appl Climatol 129:33–45 https://doi.org/10.1007/s00704-016-1747-4

Zarei AR, Shabani A, Mahmoudi MR (2019) Comparison of the climate indices based on the relationship between yield loss of rain-fed winter wheat and changes of climate indices using GEE model. Sci Total Environ 661:711–722 https://doi.org/10.1016/j.scitotenv.2019.01.204

Zhang Y, Chen W, Smith SL, Riseborough DW, Cihlar J (2005) Soil temperature in Canada during the twentieth century: Complex responses to atmospheric climate change. J Geophys Res Atmos 110 https://doi.org/10.1029/2004JD004910
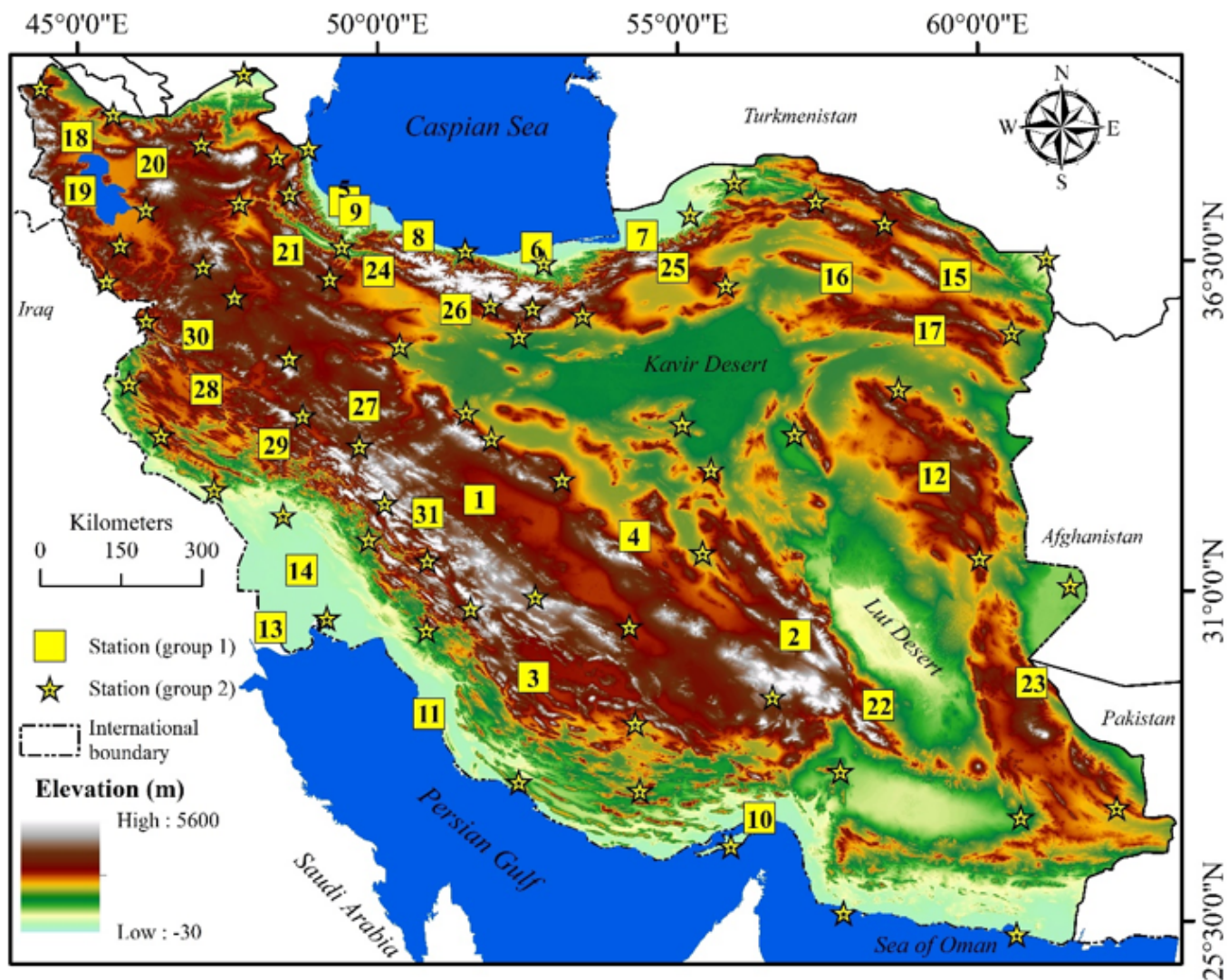
Figures

Figure 1

Locations of the studied stations and Iran's Digital Elevation Model (DEM)
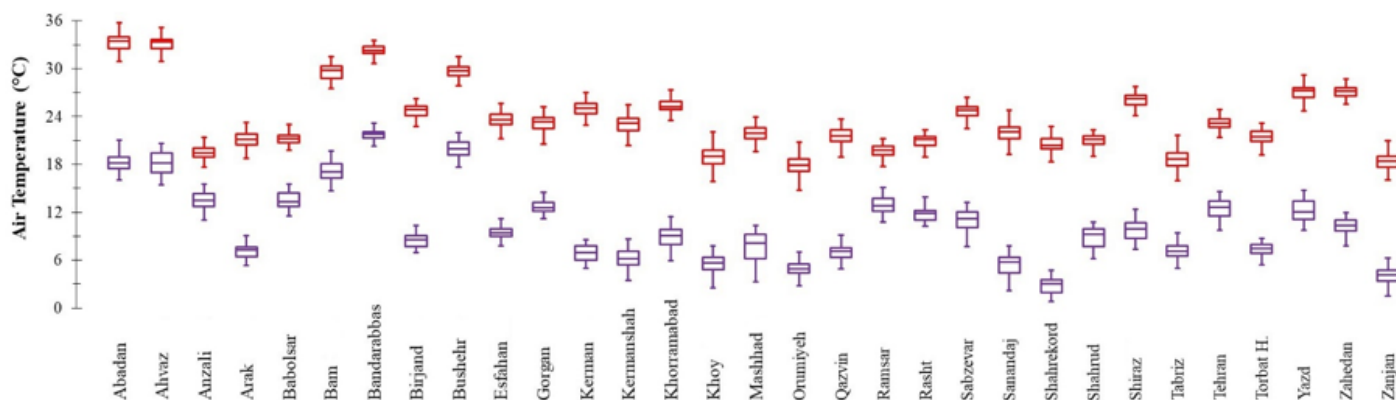

Figure 2

Tmin and Tmax box plot. Purple and red box plots indicate Tmin and Tmax, respectively
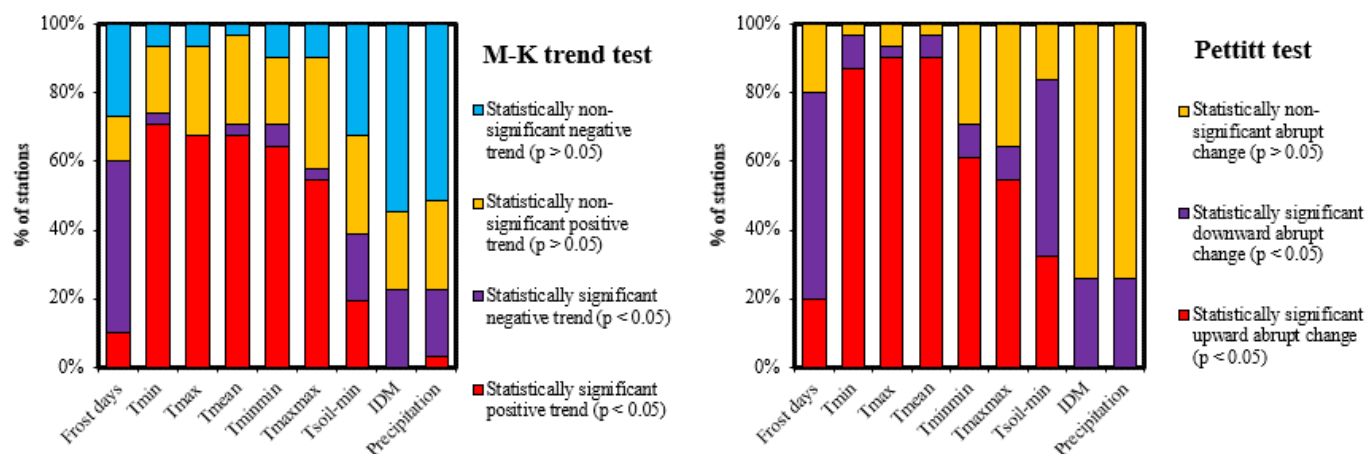

Figure 3

Percentage of stations with positive and negative trends and percentage of stations with upward and downward abrupt changes
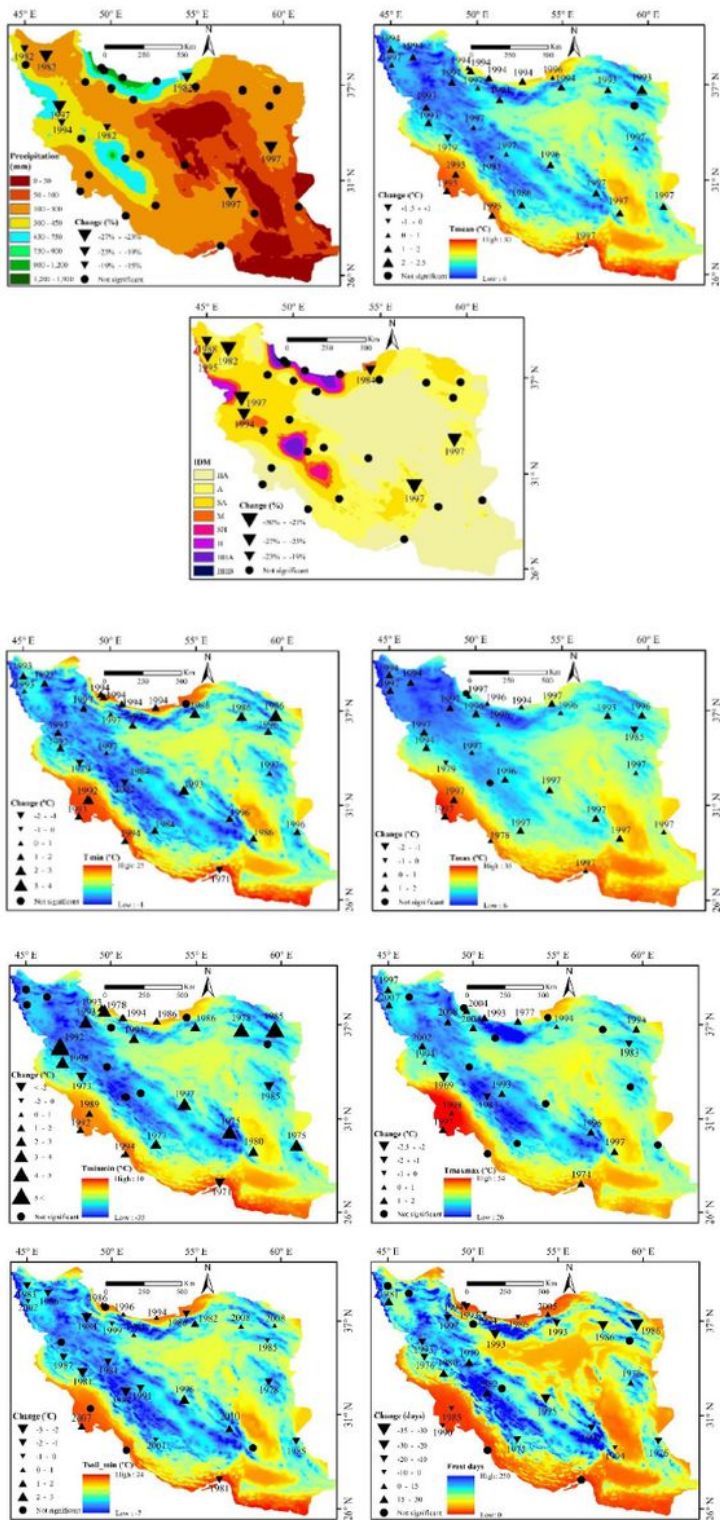
Figure 4

The average amount of the temperature indices changes for post-breakpoint compared to pre-breakpoint. Labels show abrupt change year. Background coloured maps represent the spatial distribution of each index between 2009 and 2018. Up and down pointing triangles denote upward and downward abrupt changes, respectively (p < 0.05). Also, solid circles demonstrate non-significant abrupt changes (p > 0.05)
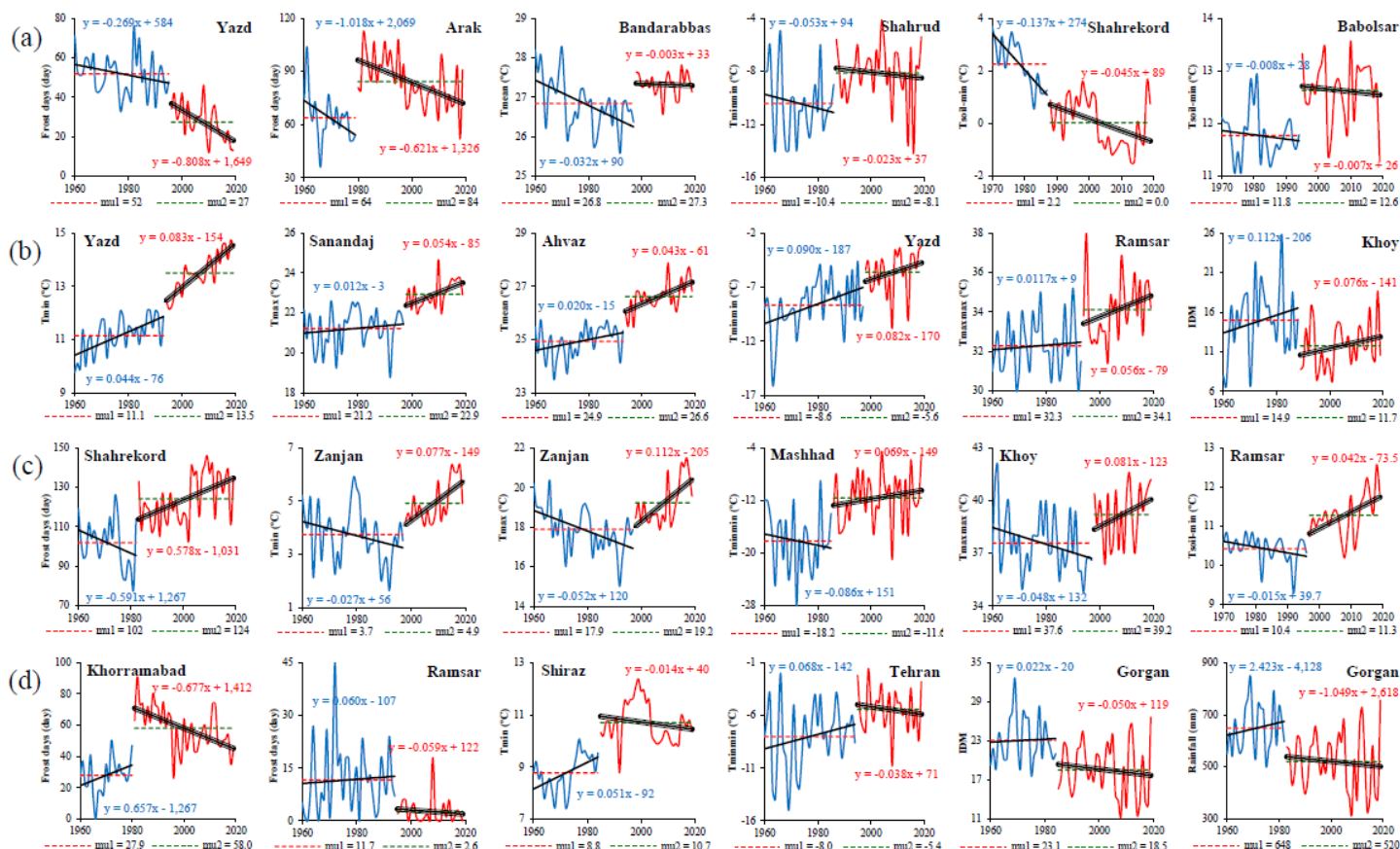
Figure 5

Time series of the selected stations with a) a decreasing trend before and after change points, b) an increasing trend before and after change points, c) a decreasing trend before abrupt changes and an increasing one afterwards, and d) an increasing trend before abrupt changes and a decreasing one afterwards
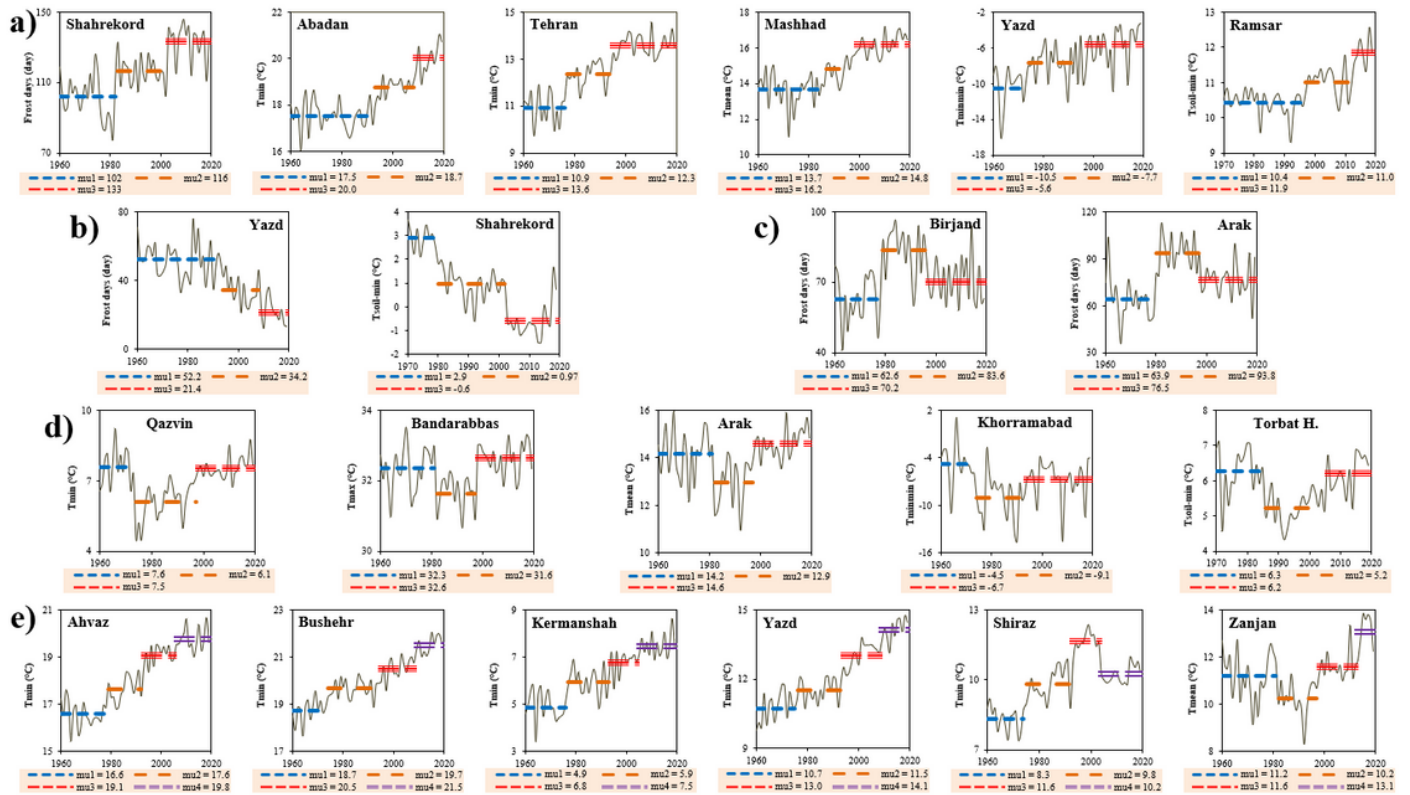
Figure 6

Time series of selected stations with a) two abrupt upward changes, b) two abrupt downward changes, c) the first abrupt change is upward and the second one is downward, d) the first abrupt change is downward and the second one is upward, and e) three abrupt changes
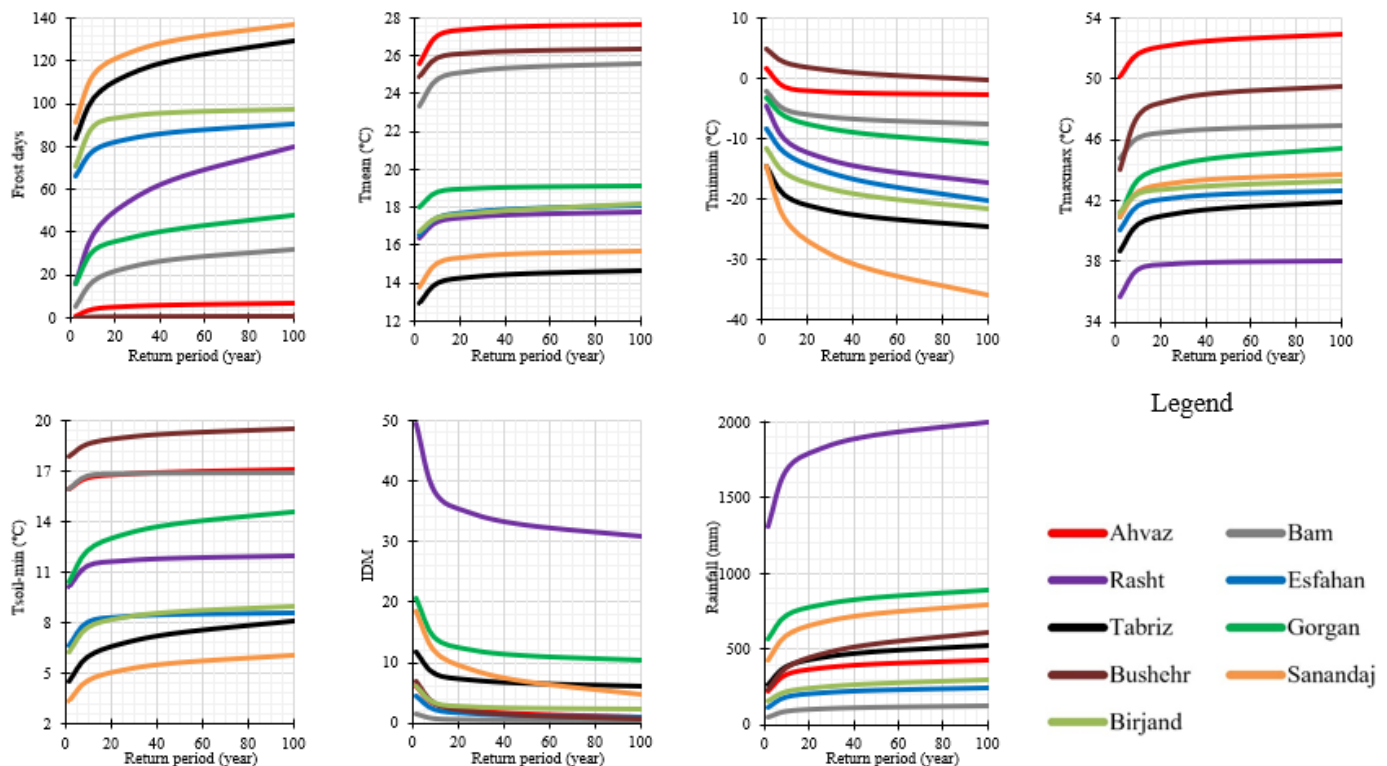
Figure 7

Return period of 9 selected stations